Highly-Selective Electronically-Tunable Cryogenic Filters Using Monolithic, Discretely-Switchable MEMS Capacitor Arrays

Eric M. Prophet, Jürgen Musolf, Betty F. Zuck, Silverio Jimenez, Kenneth E. Kihlstrom, and Balam A. Willemsen

***Abstract*—A low loss electronically tunable filter was demonstrated using HTS/Au MEMS switched capacitor arrays. The two-pole filter was tuned by simultaneously varying the capacitance of each resonator by equal amounts. A K factor of between 3,500 and 5,000 was demonstrated for single pole resonators. The total tuning range was about 25% with an average Q of 7,000 at 77 K.**

***Index Terms*—Cryogenic electronics, filters, microelectromechanical devices, tunable circuits and devices.**

I. Introduction

THE use of Micro Electromechanical Systems (MEMS) with High Temperature Superconductors (HTS) has enabled a new class of highly-selective tunable filters. HTS microstrip filters are generally planar, and are thus very well suited to subsequent monolithic processing such as MEMS technology. The object of this study is to demonstrate the compatibility of MEMS technology with the HTS processing and operating conditions, to determine to what extent normal metal MEMS over an HTS circuit can be used for tuning of a multi-pole filter, and to what extent the normal metal MEMS degrades the nominal quality factor of the original all HTS resonators.

II. MEMS Capacitor Arrays

The introduction of MEMS technology into the Radio Frequency (RF) market offers the possibility of many promising breakthroughs in a number of important areas including optical beam steering, voltage controlled oscillators, tunable patch antennae, and tunable RF filters. In the majority of these cases, some sort of RF switching constitutes the means to modify the electrical circuit. In the present case, a MEMS variable capacitor is used to alter the capacitance of an HTS resonant circuit.

Discretely Switchable Capacitors (DSC) can be made from a singly anchored cantilever beam [1], though our approach lends itself more readily to a doubly anchored beam structure since the device acts much like a switch that is nominally either *on* or *off* [2], [3]. Multiple capacitors of different values forming a tuning *bank* can provide a significant amount of capacitance change [4]. This paper focuses on our DSC array efforts and their employment as active elements in tunable HTS filters.

Manuscript received October 5, 2004. This material was based on work supported by the Defense Advanced Research Projects Agency, Defense Sciences Office, Order no. J607, Totally Agile RF Sensor Systems, issued by DARPA/CMD under Contract #MDA972-00-C-0010.

E. M. Prophet, J. Musolf, B. F. Zuck, S. Jimenez, and B. A. Willemsen are with Superconductor Technologies Inc., Santa Barbara, CA 93111 USA (e-mail: balamw@suptech.com).

K. E. Kihlstrom is with the Physics Department of Westmont College, Santa Barbara, CA 93108 USA, and also with the Superconductor Technologies Inc., Santa Barbara, CA 93111 USA.

Digital Object Identifier 10.1109/TASC.2005.850136

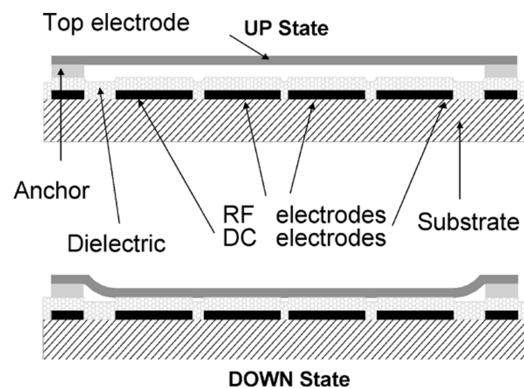

Fig. 1. Cross-section of a typical DSC. The lower RF and DC electrodes are HTS, the anchor and top electrode are gold, and the dielectric is BCB. The DSC is actuated electrostatically by application of 100–250 Vdc between the upper gold beam and lower DC electrodes.

III. Design

Fig. 1 shows a schematic view of a typical cross-section of the electrostatically actuated Discretely Switchable Capacitor (DSC) used throughout this study.

In order to maintain a high quality factor (Q) for the resonant circuit (necessary for high-selectivity filters), the materials used to fabricate the DSC depicted in Fig. 1 must be chosen carefully. In the present case, HTS (TBCCO) was used to form the resonant circuit and forms both the DC and RF lower electrodes of the DSC switch. The upper electrode was fabricated out of gold, though other suitable metals could be used. The dielectric material chosen was photoimagable Benzocyclobutene (BCB 4024). This BCB has a low loss tangent (approximately 4×10^{-4} in the frequency range of interest), is easily deposited, has a low curing temperature, little or no outgassing in vacuum, has an adequate breakdown voltage (300 $\mathrm{V}/\mu\mathrm{m}$) [5], and exhibits very little electrostatic charge trapping. The dielectric constant of BCB however, is relatively low compared with other commonly used dielectrics such as silicon nitride or strontium titanate which can be an order of magnitude higher or more.

The gold is patterned to form air-bridges above the HTS lower electrodes and BCB dielectric creating the high Q voltage controlled variable capacitors. Electrically, the beam can be modeled as two multi-dielectric series capacitors (4 μm air gap

1051-8223/$20.00 © 2005 IEEE

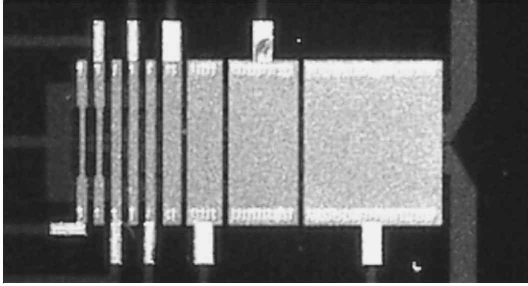

Fig. 2. Optical microphotograph of a nine-switch (512 state) capacitor array. This array has a total capacitance that varies from 0.2 pF to 2.0 pF. The largest capacitor in the array measures $800\ \mu\mathrm{m} \times 600\ \mu\mathrm{m}$ and is designed to provide 1 pF of capacitance in the downstate.

(vacuum in the present case) and 1.4 $\mu\mathrm{m}$ BCB) in the upstate, and two simple series capacitors (1.4 $\mu\mathrm{m}$ BCB dielectric) in the downstate. The active area of the beams and underlying electrodes determines their discrete values.

Fig. 2 shows a typical 9-bit array of DSC switches. The total length of each DSC switch is 800 $\mu\mathrm{m}$. The widths range from 600 $\mu\mathrm{m}$ at the largest end of the array, to 25 $\mu\mathrm{m}$ at the smallest end. The active area of the lower electrodes also varies from switch to switch in order to obtain the required capacitance values. The DSC array is designed in a standard binary fashion such that each succeeding capacitor value is half that of the previous one. The largest capacitor in the bank was designed to have an on state capacitance of 1 pF. With an initial separation gap of 4 $\mu\mathrm{m}$, the off state capacitance of the largest switch should be approximately 0.1 pF providing an on to off capacitance ratio of 10:1.

The array of DSC switches shown in Fig. 2 was patterned monolithically over the gathered ends of a half-wave HTS microstrip resonator. The pull-down voltage was between 150 and 250 Vdc depending on the actual thickness, the amount of residual stress in the beam, and is independent of the width (i.e. the capacitance value) of the particular beam [6]. The entire switch array with these dimensions, separation distances and choice of dielectric was therefore capable of producing a total change in capacitance of approximately 1.8 pF. By switching various combinations of the 9 switches in and out of the circuit, a digital response of 512 discrete and very reproducible capacitance states can be achieved.

IV. Fabrication

All of the fabrication steps relating to the MEMS structures and processes must be compatible with the underlying HTS materials and processes. Traditional MEMS materials such as silicon, nitrides and oxides are not compatible since they are lossy and most often require elevated deposition temperatures that might damage the HTS. Metallization methods such as electroplating are difficult as the baths often attack the HTS and degrade its performance. Since the device must be operated at cryogenic temperatures (typically 77 K), even small mismatches in thermal expansion coefficients in the MEMS can have a dramatic effect on the structure upon cooling.

After patterning the HTS resonant circuit on a magnesium oxide substrate (MgO), a 1.4 $\mu\mathrm{m}$ thick BCB dielectric/passivation layer is deposited over the entire HTS circuit. Vias are opened in the BCB to facilitate contact to RF and DC input/output connections. A 4 $\mu\mathrm{m}$ thick sacrificial photoresist release layer is then deposited and vias are patterned to gain access to the same I/O connections on the substrate. The electrical skin depth of the active metal forming the upper electrode dictates its thickness, 3–4 $\mu\mathrm{m}$ of gold in the present case, which is sputtered over the photoresist release layer and patterned to form the beams. These beams are anchored to the substrate through the vias patterned previously in the photoresist. Careful attention must be paid to the sputtering deposition conditions to minimize the residual stress in the thin films, and to avoid excessive heating of the underlying photoresist. The sacrificial photoresist is then stripped and the beams are released in an Alkane-thiol solution to help reduce stiction [7].

V. Experimental Results

The HTS resonator with the 9-bit DSC array as shown in Fig. 2 was fabricated and the frequency shift (tuning) due to changing capacitance values was measured using an HP-8720 vector network analyzer. The high side of the DC bias is applied to one of the two anchors on each switch by means of an extended HTS microstrip transmission line. The lower HTS DC electrode is held at DC ground, also by means of an extended HTS microstrip transmission line. Wideband RF chokes are used at the DC ports of each switch to minimize losses. The transmission lines are wire bonded to a 19 pin Molex connector with Manganin wire feed-throughs to allow DC access in and out of the evacuated cryostat.

The design capacitance ratio for the MEMS with these dimensions was 10:1. In practice, small variations in actual release layer thickness will limit the working capacitance ratio. Due to the nature of the monolithic process, the beam is not precisely conformal with respect to the substrate and underlying circuit. This is due to *print-through*, which occurs frequently as the beam metal is deposited over partially planarizing BCB, and sacrificial photoresist layers that cover the underlying electrodes. Since the topography of the beam and the underlying circuit are not precisely conformal, the beams often cannot make intimate contact with the underlying structure. We believe that these process variations are partially responsible for the noticeable decrease in the design capacitance ratio from 10:1 to an actual working ratio of about 6:1.

Fig. 3 shows the frequency shifts resulting from the individual capacitance states realized using the single-pole hairpin resonator and 9-bit capacitor array described above. The DSC's are individually addressed via a high-voltage controller using programmable TTL signals and a standard PC. All of the 512 distinct frequency states are shown in Fig. 4. The total tuning range for this device is roughly 25% (125 MHz of a 500 MHz average center frequency). The Q of the HTS circuit in the absence of the MEMS is approximately 25 000. The introduction of the MEMS can lower the initial resonator Q by as much as 50%. As the resonator is tuned farther from its design frequency and more energy is being stored in the lossier MEMS, the Q of the circuit is degraded still further.

The figure of merit associated with this type of tuning is known as the K factor, and is expressed as a function of the

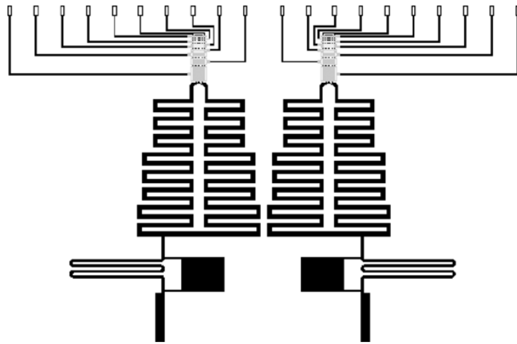

Fig. 3. AutoCAD drawing of the HTS 2-pole constant bandwidth filter with tandem 9-bit MEMS capacitor arrays. 18 DC bias connections are shown at the top, and resonant I/O RF coupling structures are shown at the bottom.

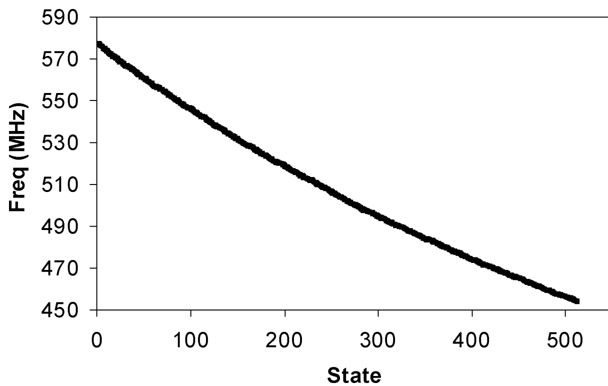

Fig. 4. Frequency versus state for an HTS tunable resonator using a 9-bit MEMS capacitor array. All 512 states can be identified in the data. The total circuit Q at 77 K (including the MEMS) varies from $\sim$12 000 at high frequencies to $\sim$2,000 at lower frequencies.

tuning percentage and average quality factor of the tunable circuit: $K = 2 \cdot Q \cdot (\Delta f / f_0)$ where $\Delta f / f_0$ is the tuning percentage with respect to the average center frequency of the resonator. The K factor for this device ranged from about 3,500 to as high as 10 000 depending on the quality of the particular HTS film and the operating temperature of the device. These K values are perhaps two orders of magnitude higher than those obtained using other tuning methods such as tunable dielectrics [8].

We found that the relatively high actuation voltages necessary to actuate the 3–4 μm thick beams in the absence of any gas damping created undesirably high contact forces which lead to premature mechanical failures in the MEMS. Altering the waveform of the drive signal effectively slowed the switching speed from on the order of 100's of microseconds to on the order of 10's of milliseconds and eliminated this self-destructive behavior.

Continued temperature cycling can overstress the metal in the beams and lead to beam warping, which can adversely affect the capacitance value and possibly the actuation voltage of the device, rendering individual capacitors much less "discrete" with respect to their contribution to the total capacitance of the array.

VI. Tunable Filters

To demonstrate the accuracy with which the MEMS can control the resonant frequency of a multi-pole filter, a two-pole bandpass filter was designed with a constant bandwidth of 1 MHz (measured 1.0 dB below the passband insertion loss minimum) across the entire tunable frequency range [9]. This microstrip style HTS filter was modified with the monolithic MEMS arrays as shown in the AutoCAD drawing in Fig. 4, and was tested in vacuum at 77 K.

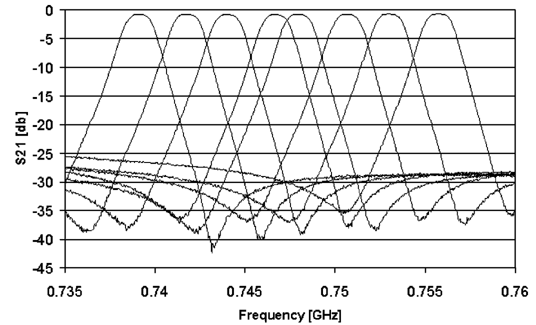

Fig. 5. 8 different transmission response (S_{21}) curves of a MEMS tuned constant bandwidth 2-Pole HTS microstrip filter. Each trace represents a different capacitance setting. The states in the figure are (from right to left): 0, 2, 4, 6, 7, 9, 11, & 13. A total of 18 switches control the capacitance of each of the two poles. The filter shape and designed bandwidth is preserved.

The HTS/MEMS hybrid filter was tested in a microwave enclosure using sapphire fine-tuning elements above each resonator to pre-balance the two-resonator structure. This one-time balancing step compensates for slight physical differences in the resonators due to processing variations from run to run, and helps to optimize the insertion loss. After balancing the structure, the sapphire tuners are locked in place. Each resonator of the balanced filter was then tuned independently using two identical arrays of nine DSC switches. To keep the bandwidth constant, even small changes in capacitance on one side of the filter must be matched with an identical capacitance change on the opposite side to maintain the proper balance. Fig. 5 is a plot showing some of the transmission responses generated by the MEMS tuned 2-pole filter. Each S_{21} response was generated using a different capacitance value (state) on each array and was measured using an HP-8753 vector network analyzer. As is shown in the figure, the bandwidth does remain constant as the filter is tuned from one state to the next, indicating that the DSC MEMS arrays are providing adequate precision on both sides of the filter. The filter was tuned between 755 MHz and 580 MHz with $\sim$500 kHz resolution and exhibited remarkably good bandwidth control across the entire tuning range.

VII. Loss Mechanisms

The hybridization of the Au/BCB on HTS introduces losses due to the resistance of the overlaying materials. Gold was chosen as the upper electrode due to its superior electrical properties, and for its mechanical properties at both room and cryogenic temperatures. The BCB dielectric of the MEMS capacitor is a major contributor to the overall loss of the resonant circuit, and a small amount of loss can be attributed to the BCB passivation layer (we measured less than 1% change with and without 1.4 μm of BCB over the resonator). Since literature data for the loss tangent of BCB was only available for frequencies between 1 kHz to 1 MHz (8×10^{-4}) and at room temperatures, we measured the loss tangent of lifted-off

polymer samples in the temperature and frequency range of interest and found it to be 4×10^{-4}.

The insertion loss of the system with all 18 DSC's in the off state (untuned) is less than -0.7 dB. As the filter is tuned farther away from the untuned state, the insertion loss of the filter begins to degrade reaching almost -5 dB at the fully tuned state. This can be attributed to changes in the external coupling, energy loss through the DC biasing, and the increase in the energy being stored in the MEMS.

One approach to reducing some of the losses associated with the dielectric is to reduce the *dielectric fill factor* by patterning the portions of photoimagable BCB over the RF electrodes. While this approach produced only marginal improvements in Q (less than 30% with a fill factor of 0.35), it did help to greatly reduce the static and dynamic stiction in the device. Cooling the devices below 77 K also provided measurable improvements in Q. This improvement was found to be primarily due to the decrease in the resistance of gold and not due to the BCB.

VIII. Conclusion

The MEMS technology was used to fabricate an array of low loss switches that are capable of precise capacitance changes enabling electronic control of a highly selective HTS multi-pole filter. Binary addressable arrays of discretely switchable capacitors using cryogenically compatible materials were fabricated and tested, specifically; gold beams suspended over HTS electrodes with a BCB dielectric on an MgO substrate.

A highly selective constant bandwidth bandpass filter was used as a test bed for the MEMS array. The 2-pole HTS filter was designed with a constant bandwidth of 1 MHz. The MEMS tuning arrays were designed with 500 kHz average resolution. A total tuning range of 25% was realized with an initial insertion loss less than 0.7 dB for the entire circuit. The insertion loss remained above -1.0 dB through about the first 10% of the tuning range and fell to below -4 dB at the highest capacitance state.

The normal metal and dielectric materials used to form the bulk of the capacitors degraded the Q of the HTS circuit substantially, particularly as more and more energy was being stored in the lossy dielectric. However, the average Q of the circuit including the MEMS of 7,000 is still orders of magnitude higher than typical Q's for conventional devices at these frequencies. The losses are primarily due to the lossy BCB and the gold metal bridges in the MEMS. Losses can be reduced in the HTS/normal-metal hybrid using methods such as dielectric patterning in the MEMS, thinning or removing the passivation layer over the resonators, and by lowering the operating temperatures, though these improvements are perhaps a factor of 2 and not orders of magnitude.

Acknowledgment

The authors would like to thank G. L. Matthaei, G. L. Hey-Shipton, K. F. Raihn, J. Fuller, R. M. Whirty, M. Hernandez, P. A. Kohl, C. J. Kim, R. C. Eden, J. E. Mancusi, M. W. Roberson, C. K. Williams, D. J. Scalapino, and R. B. Hammond for many useful interactions relating to this work.

References

[1] A. K. Chinthakindi, D. Bhusari, B. P. Dusch, J. Musolf, B. A. Willemsen, E. M. Prophet, M. Roberson, and P. A. Kohl, "Electrostatic actuators with intrinsic stress gradients," *J. Electrochemical Soc.*, vol. 149, no. 8, pp. H139–H145, 2002.

[2] Y. S. Hijazi, D. Hanna, D. Fairweather, Y. A. Vlasov, and G. L. Larkins Jr., "Fabrication of a superconducting MEMS shunt switch for RF applications," *IEEE Trans. Appl. Supercond.*, vol. 13, no. 2, Jun. 2003.

[3] J. Muldavin and G. M. Rebeiz, "All-metal high-isolation series and series/shunt MEMS switches," *IEEE Microw. Compon. Lett.*, pp. 59–71, Dec. 2001.

[4] N. Hoivik, M. A. Michalicek, Y. C. Lee, K. C. Gupta, and V. M. Bright, "Digitally Controllable Variable High-Q MEMS Capacitor for RF Applications," NSF Center for Advanced Manufacturing and packaging of Microwave, Optical and Digital Electronics, Dept. of Mechanical Engineering, Univ. Colorado, Boulder, CO. MTT-S01.

[5] D. Scheck, "CYCLOTENE (BCB) resins for wafer bumping and wafer level packaging," in *WLP Seminar*, Hsinchu, Taiwan, Sep. 14, 2001.

[6] H. Nieminen, V. Ermolov, K. Nybergh, S. Silanto, and T. Ryhänen, "Microelectromechanical capacitors for RF applications," *J. Micromech. Microeng.*, vol. 12, pp. 177–186, 2002.

[7] R. Maboudian, W. R. Ashurst, and C. Carraro, "Self-Assembled Monolayers as Anti-Stiction Coatings for MEMS: Characteristics and Recent Developments," Dept. of Chemical Engineering Univ. California Berkeley.

[8] B. H. Moeckly, L. S.-J. Peng, and G. M. Fisher, "Tunable HTS microwave filters using strontium titanate thin films," *IEEE Trans. Appl. Supercond.*, vol. 13, no. 2, Jun. 2003.

[9] G. .36+-L. Matthaei, "Narrow-band, band-pass filters with zig-zag, hairpin-comb resonators," in *IEEE-MTT-S Dig.*, 2002, pp. 1931–1934.